Rock and Soil Mechanics

Volume 43 | Issue 8 Article 5

10-9-2022

Slope stability of an unsaturated embankment with and without natural pore water salinity subjected to rainfall infiltration

SADEGHI Hamed

KOLAHDOOZ Ali

AHMADI Mohammad-Mehdi

Custom Citation

SADEGHI Hamed, KOLAHDOOZ Ali, AHMADI Mohammad-Mehdi. Slope stability of an unsaturated embankment with and without natural pore water salinity subjected to rainfall infiltration[J]. Rock and Soil Mechanics, 2022, 43(8): 2136-2148.

Rock and Soil Mechanics 2022 43(8): 2136−2148 ISSN 1000−7598
https: //doi.org/10.16285/j.rsm.2021.00155 rocksoilmech.researchcommons.org/journal

Slope stability of an unsaturated embankment with and without natural pore water salinity subjected to rainfall infiltration

SADEGHI Hamed, KOLAHDOOZ Ali, AHMADI Mohammad-Mehdi

Department of Civil Engineering, Sharif University of Technology, Tehran 1458889694, Iran

Abstract: Natural soils contain a certain amount of salt in the form of dissolved ions or electrically charged atoms, originated from the long-term erosion by acidic rainwater. The dissolved salt poses an extra osmotic water potential being normally neglected in laboratory measurements and numerical analyses. However, ignorance of salinity may result in overestimation of stability, and the design may not be as conservative as thought. Therefore, this research aims to first experimentally examine the influence of pore water salinity on water retention curve and saturated permeability of natural dispersive loess under saline and desalinated conditions. Second, the measured parameters are used for stability analyses of a railway embankment in an area subjected to regional rainfall incident. Eventually, a numerical parametric study is carried out to explore the significance of different rainfall schemes, construction patterns, and anisotropic permeability on the factor of safety. Results reveal that desalinization suppresses the water retention capability, which in turn results in a tremendous declination of unsaturated hydraulic conductivity. Despite the natural saline embankment, rainfall can hardly infiltrate into the desalinated embankment due to the lower conductivity. Therefore, the factor of safety for natural saline conditions drops notably, while only marginal changes occur in the case of the desalinated embankment.
Keywords: slope stability; water salinity; osmotic potential; dispersive loess; rainfall patterns

1 Introduction

Rainfall is considered one of the main causes of serviceability and failure of slopes, whether they are natural or man-made slopes, such as railway embankments[1]. Such slopes are in unsaturated states, and the stability conditions are satisfied by additional suction stress unless an anticipated rainfall is heavy enough to vanish most of the inter-particle suction stress chains[2]. Consequently, the shear strength decreases and the geotechnical infrastructure will fail and become unstable[3]. Because of its utmost importance, remarkable interdisciplinary research has been devoted to the stability of geostructures subjected to rainfall by adopting various methodologies and site specific conditions. The majority of previous research on slope stability assumed, however, that the pore fluid permeating through the soil voids is pure or distilled water with virtually no osmotic potential. This is certainly not the case where dissolved ions in pore water are abundant because they can affect both the water flow regime, and stability conditions[4–5].

There has recently been increasing growth in the experimental research on the influence of molar concentration or pore water salinity on both mechanical and hydraulic behaviour of soils, including swelling potential and the soil-water retention properties[6–7]. For instance, it has been investigated that the molar concentration can dramatically influence the volume change behavior of active clays, causing them to act like non-active materials[8–9]. However, most of these works have be done in the saturated conditions and none of them consider the unsaturated condition for soil. Also, it should be noted that most of these studies focused on the behaviour of expansive soils, and much less attention has been given to the collapsible soils. Results of some experimental research revealed that existence of salt in the pore water could enhance the retention capability of soils based on this fact that salinity produces osmotic suction in addition to the matric potential[10–12]. Garakani et al.[13] revealed that depending on the type of mineral of the salt, the increament of retention capability can vary differently. On the other hand, it is known that for the same suction values, the more the retention ability, the higher the rate of the unsaturated hydraulic conductivity[14–15]. In other words, salinity can indirectly have an influence on the unsaturated hydraulic conductivity and can improve it by rising the water phase region within the soil structure.

Dispersive soils also categorized as a kind of problematic soils for construction purposes comprise of notable dissolved salts depending on their dispersive potential. Even though the general recommendation is to avoid using this type of soil or to improve them [16], especially where catastrophic outcomes are expected (such as in the core of earthfill dams), budget constraints may not always allow following this protocol. For example, parts of a mega railway project connecting Chabahar port to the international rail network had to cross natural dispersive strata with high dispersive potential[17]. Chabahar port and the study area, as shown in Fig. 1, are located at the most east southern Iran. According to Fig. 1(a), the study area has a semi-arid climate with relatively low annual rainfall, but sometimes has sudden stormwaters. The hydrology of this region is compared for the two exemplified wet and dry seasons in Figs. 1(b) and 1(c),

Received: 20 December 2021 Revised: 10 March 2022
First author: SADEGHI Hamed, male, born in 1983, PhD, Assistant Professor, mainly focused on multiphysics of natural and engineered soils. E-mail: hsadeghi@sharif.edu

respectively. The consequence can appear in the form of structural damages to nearby infrastructures. As shown in Fig. 2, severe stability problems occurred in the railway embankment after the rainfall incident in March 2019. Therefore, some insight into the behaviour of such soils seems necessary to prepare for appropriate countermeasures for similar geological conditions in the future. It is also worth noting that soils generally contain a certain amount of dissolved ions and salts as a natural consequence of erosion and weathering especially by precipitation of acidic rainfall.

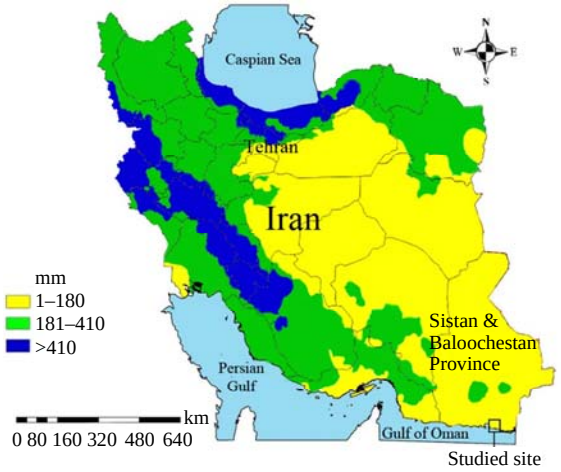

(a) Location of the studied site on rainfall infiltration map of Iran

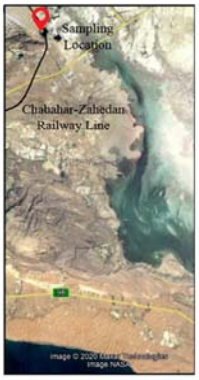

(b) Hydrological conditions during wet season

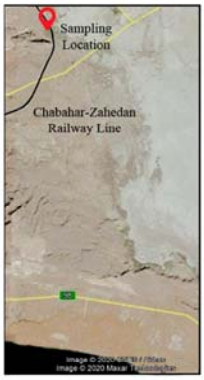

(c) Hydrological conditions during dry season

Fig. 1 Chabahar port and study area

Fig. 2 Severe stability problems occurred at the studied railway embankment after a high rain season during the Spring of 2019

The main objective of this study is to investigate the effect of natural salinity on the stability of an unsaturated railway embankment under rainfall infiltrations. To achieve this objective, water retention and hydraulic characteristics of the in-situ soil are measured and estimated along the wetting path simulating the rainfall incident for natural saline and artificial desalinated soil conditions. Laboratory measurements are used as input parameters for seepage and stability analyses in numerical modelling. The numerical simulations also include a parametric study to investigate the influence of construction patterns, rainfall intensity, and anisotropy of the hydraulic conductivity on the stability.

2 Experimental study

2.1 Test materials

For the purpose of studying the effect of natural salt on the soil-water retention curve (SWRC) and the unsaturated hydraulic conductivity function, natural dispersive loess in block samples were retrieved from a test pit at the study area shown in Fig. 1. The soil having an in-situ dry density and water content of 1 153 kg/m^3, and 14.2%, respectively, is classified as a lean clay. Moreover, results of chemical tests revealed that the studied material was moderately to highly dispersive, with sodium being the major cation. Detailed information on other classification and geotechnical characterization can be found in Sadeghi et al. [4]. Therefore, one type of test material was directly retrieved soil with natural salinity. Another type was obtained by desalinization of the natural soil to several cycles so that a considerable amount of salt could be washed out. Details of the desalinization process and the consequent verification results will be presented in the following section.

In addition to pore water salinity as a key variable in this study, test specimens were prepared at two states of compaction to reliably mimic the conditions of the natural soil stratum and the railway embankment. The first state of compaction, namely *Natural Compaction State* resembles the natural state of the stratum with the in-situ dry density ρ_d of 1 153 kg/m^3 corresponding to a void ratio e of 1.39. The second state of compaction called *Standard Compaction State* throughout the paper simulates the general compaction condition of the railway embankment. According to the *National earthworks code for railway lines*[18], a compaction ratio of 90% is adopted, corresponding to a dry density of 1 485 kg/m^3 or a void ratio of 0.85. In summary, four types of test material were prepared and examined in both laboratory and numerical investigations. The material identities and corresponding conditions from the viewpoints of compaction and salinity conditions are summarized in Table 1.

Table 1 Four types of material used in this study

ID	Salinity state	Compaction state	ρ_d /(kg • m^{-3})	e	k_{sat} /(m • s^{-1})	φ' /(°)	c' /kPa
SaNa	Saline	Natural	1 153	1.39	8.7×10^{-8}	28.9	0
SaSt		Standard	1 485	0.85	1.1×10^{-8}	29.1	7
DeNa	Desalinated	Natural	1 153	1.39	8.5×10^{-8}	28.9	0
DeSt		Standard	1 485	0.85	8.1×10^{-9}	29.1	7

Note: k_{sat} is saturated hydraulic conductivity, φ' is effective internal friction angle, c' is effective cohesion.

2.2 Desalinization process and sample preparation

As mentioned earlier, in order to remove the natural pore water salinity from the in-situ soil, the desalinization procedure introduced by Zhang et al. [19] was adopted. Following this method, the natural soil was thoroughly mixed with deionized distilled water with a ratio of 1 to 5 for soil and water, respectively. Afterwards, the mixture was poured in a graduated cylinder for sedimentation for 24 h; thereafter, the clear portion of the solute was poured out carefully by using a hypodermic syringe. This procedure was repeated with fresh distilled water until a significant reduction in salinity was reached. In order to quantify the salinity, the electrical conductivity of the solute was measured with an electrical conductivity meter after each desalinization cycle. Fig. 3 shows the results of electrical conductivity measurements during the desalinization process. According to the results, the initial electrical conductivity of the solute was 3.87 mS/cm and dropped significantly to a value as low as 0.1 mS/cm at the 7th cycle. In addition, the rate of changes in the electrical conductivity reduces towards final desalinization cycles, suggesting an asymptotic value corresponding to the last cycle. In other words, negligible reduction in pore water salinity can be expected by further desalinization. As a result, the soil slurry at this stage was oven-dried and considered as the desalinated material in this study.

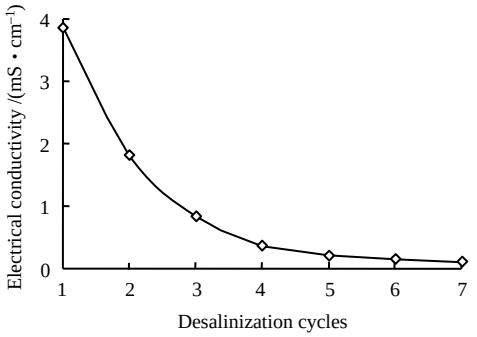

Fig. 3 Monitoring of desalinization process based on the measurement of electrical conductivity

In order to measure water retention curves of saline and desalinated soils in both natural and standard compaction states, a total of 36 test specimens was prepared with a height of 34 mm and a diameter of 46.3 mm. All the specimens were statically compacted inside cylindrical molds at the rate of 0.5 mm/min by an electrical loading jack following the procedure described by Sadeghi[20]. In order to include measurements of the osmotic potential, three Whatman #42 standard filter papers were incorporated to measure both total, and matric suctions in each specimen. In addition, all specimens were compacted with an in-situ water content of 14.2% in two layers while the contact filter paper within two ordinary filter papers was sandwiched between them. After static compaction to the target dry densities, all the specimens were placed in an oven for 24 hours to be completely dried. The predetermined amount of distilled water corresponding to a uniform distribution of the volumetric water content was added to each specimen by using a pipette dropping glass tube. It should be noted that distilled water was used as the wetting liquid because the rainfall was considered to be pure, and independent of the salinity level of the soil stratum. After the specimen moistening process, two non-contact filter papers were placed on top of the specimen with a buffered plastic mesh in between. The specimens were then wrapped in several consecutive layers of cling and aluminium foils, and placed in an ice chest inside the humidity-controlled compartment of the laboratory for an equilibrium period of one month. Eventually, according to the ASTM-D5298[21], all filter papers and the specimens were weighed in both moist and oven-dried conditions in order to calculate the soil–water retention data.

2.3 Soil–water retention tests

In order to reliably mimic the rainfall incident applied on a railway embankment, all water retention tests were conducted along the wetting path and the influence of stress was neglected because of the low overburden pressure induced by the shallow embankment[22]. It is worth mentioning that capillary phenomena corresponding to the matric component of suction dominates the hydro-mechanical behavior of unsaturated soils under low suction regime. This is true if the osmotic component of pore fluid and boundary flux fluid is essentially the same. Otherwise, there will be a flow from low concentration to high concentration regime because of the differences in osmotic suction even under the same matric suction. Therefore, to explore the significant role of dissolved salts into the pore fluid on flow characteristics and corresponding stability conditions, total suction-SWRC was measured and employed in this study. There is no need to mention that rainfall was considered as pure water with no osmotic suction permeating through soil pore fluid with a high TDS (total dissolved salts) or inherent osmotic suction. After measurements of the soil–water retention data, Eq. (1) suggested by Pham et al.[23] and Golaghaei et al.[24] was used to produce continuous curves from discretized and limited

measuring points as follows:

$$\theta(\psi)=\left\{\left[\theta_{\mathrm{sat}}-S_1\lg\psi-\theta_{\mathrm{r}}\right]\frac{a}{\psi^b+a}+\theta_{\mathrm{r}}\right\}\cdot\left[1-\frac{\ln\left(1+\frac{\psi}{\psi_{\mathrm{r}}}\right)}{\ln\left(1+\frac{10^6}{\psi_{\mathrm{r}}}\right)}\right] \quad (1)$$

where ψ is the soil suction, $\theta(\psi)$ is the volumetric water content corresponding to ψ, θ_{sat} is the saturated volumetric water content, θ_{r} is the residual volumetric water content, S_1, a and b are fitting parameters, and ψ_{r} is a constant related to the matric suction corresponding to the residual water content. All the measured data points of four SWRCs were used to find the best-fit model parameters of Eq. (1). The results in terms of model parameters are summarized in Table 2. Afterwards, adequate number of data points were selected along the four smooth best-fit water retention curves and the data were manually defined in the simulation software thorough "Data Point Function". As a result, the same water retention curves obtained from Eq. (1) were used for flow analysis.

Table 2 Values of fitting parameters adopted for the SWRCs

Material	θ_{sat} /%	θ_{r} /%	S_1	a	b	ψ_{r} /kPa
SaNa	58.23	7.14	0.001	80.03	0.674	684.28
SaSt	55.13	20.54	0.000	5×10^7	2.544	1 391.04
DeNa	58.81	21.18	0.000	57.64	1.019	41.43
DeSt	51.03	18.74	0.000	98.23	0.972	69.59

Figure 4 shows the SWRCs of saline and desalinated soils at both natural and standard compaction states, BF means best fit, FP means fitter paper. Fig. 4(a) compares SWRCs of saline and desalinated soils for the natural compaction. According to the results, the saline soil has higher retention capability compared with the desalinated soil at the same void ratio, indicating the significant contribution of osmotic potential in water retention characteristics. In other words, the difference between the SWRCs of saline and desalinated soils arises from the osmotic suction. On the other hand, the opposite trend was reported for the matric SWRCs of a synthesized collapsible soil with changing osmotic potential [25]. The discrepancy arise from different suction components considered for the interpretation in the two studies. In other words, if the SWRC data are interpreted in terms of total suction, a soil specimen with higher osmotic suction would have a higher retention capability. Regarding high suction ranges, the results of Fig. 4(a) reveal that differences almost vanish at a relatively higher range of suction beyond 10 000 kPa. The implication is that the retention properties are similar in spite of extreme salinity levels. It has to be mentioned that discrepancies between the best-fit curves at this range is due to the nature of mathematical formulation of Eq. (1). Nonetheless, measured data points follow more or less the same trend at high suctions. In addition, this range of suction does not considerably influence the infiltration process as being far from the initial suction and the capillary-dominant regime.

Figure 4(b) indicates the SWRCs of saline and desalinated soils at the compaction state corresponding to the standard Proctor compaction effort. According to the results, SWRC of the saline soil lies above the corresponding desalinated curve for the entire range of suction due to the induced osmotic potential in saline loess. This observation is also confirmed by the previously published research[10–12]. Results of Fig. 4(b) also show that the difference between the SWRCs are not the same in the entire range of suction, suggesting that the influence of osmotic suction tends to vanish towards extreme suction levels. Comparison between the results of Figs. 4(a) and 4(b) indicates that the difference between measured SWRCs with and without pore water salinity becomes more pronounced as void ratio decreases. In other words, a reduction in void ratio enhances the clay–salt water interactions and hence magnifies the role of osmotic potential on water retention behaviour.

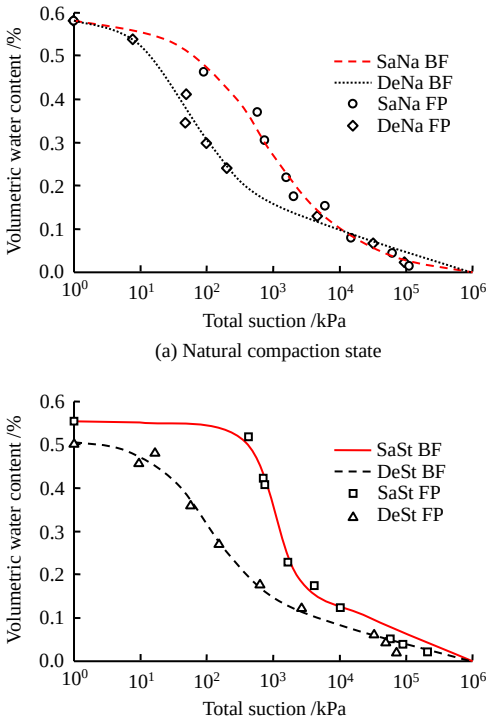

Fig. 4 Soil–water retention curves of the saline and desalinated soils

Concurrent measurements of both matric and total components of suction allow inferring the third component, which is osmotic suction. Fig. 5 represents soil water retention in terms of osmotic suction for both natural and standard compaction state. According

to the results, the key finding is that the osmotic suction is not constant for the entire range of saturation state; indeed, it increases with desaturation up to a limiting degree of saturation, and there is a sharp reduction to almost zero with a further decrease in the degree of saturation. In other words, a "belly shape" trend for variations in the degree of saturation against osmotic potential is observed for both cases. However, the limiting degree of saturation corresponding to the maximum osmotic potential is a function of compaction characteristics as a higher peak osmotic suction corresponding to a lower limiting degree of saturation is measured for the elevated compaction effort. It is noted that the limiting degree of saturation seems to be the same as the residual water content. This genuine behaviour, being rarely measured and reported in the literature, could be justified based on the fact that due to the serious lack of water in the high range of suction, dissolved salts start to crystallize and transform to be a part of solid skeleton. As a result, no osmotic potential is expected to be induced by solid salt crystals. More importantly, the range of water content below the residual value is known as the dominating adsorption mechanism regime where water exchange generally occurs through vapour transfer and the role of capillary mechanism almost vanishes [26–27].

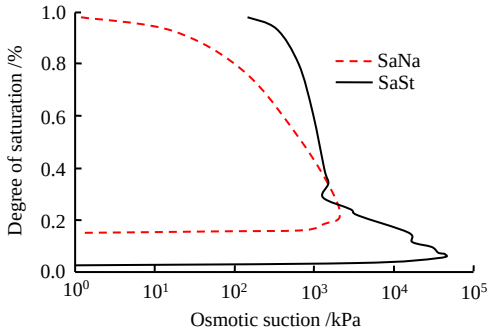

Fig. 5 Osmotic suction of saline samples in natural and standard compaction states

2.4 Unsaturated hydraulic conductivity functions

The unsaturated hydraulic conductivity function is an inevitable input variable for carrying out the water flow analysis through unsaturated soils under both steady-state and transient seepage [28]. In this study, the unsaturated hydraulic conductivity functions are estimated based on the corresponding SWRCs and the measured saturated hydraulic conductivity of test materials[29]. Recent advancement on rigorous measurement of hydraulic conductivity revealed that the adopted testing method could also affected the saturated hydraulic conductivity of problematic soils[30]. Nevertheless, a standard method was employed in this study to obtain this soil property. Indeed, the saturated hydraulic conductivity of four materials examined was measured by the falling head test method for fine-grained soils based on ASTM-D5856 [21] and summarized in Table 1. The adopted unsaturated relationship is defined as:

$$k_{\mathrm{w}} = k_{\mathrm{s}} \frac{\sum_{i=j}^{N} \frac{\Theta(\mathrm{e}^{y}) - \Theta(\psi)}{\mathrm{e}^{y_i}} \Theta'(\mathrm{e}^{y_i})}{\sum_{i=1}^{N} \frac{\Theta(\mathrm{e}^{y}) - \Theta_{\mathrm{s}}}{\mathrm{e}^{y_i}} \Theta'(\mathrm{e}^{y_i})} \tag{2}$$

where k_{w} is the unsaturated water conductivity (m/s), k_{s} is the measured saturated conductivity (m/s), Θ_{s} is the volumetric water content, e is the Euler's number equal to 2.718 28, y is a dummy variable of integration representing the logarithm of negative pore water pressure, i is the interval between the range j to N, j is the least negative pore water pressure to be described by the final function, N is the maximum negative pore water pressure to be described by the final function, ψ is the suction corresponding to the j^{th} interval, and Θ' is the first derivative of Eq. (3).

$$\Theta = \frac{\Theta_{\mathrm{s}}}{\left\{\ln\left[e + \left(\frac{\psi}{a}\right)^{n}\right]\right\}^{m}} \left[1 - \frac{\ln\left(1 + \frac{\psi}{\psi_{\mathrm{r}}}\right)}{\ln\left(1 + \frac{10^{6}}{\psi_{\mathrm{r}}}\right)}\right] \tag{3}$$

where a is approximately the air-entry value of the soil, n is a parameter that controls the slope at the inflexion point in the volumetric water content function, and m is a parameter that is related to the residual water content. It has to be mentioned that the hydraulic conductivity functions were estimated according to the defined water retention curves (Eq. (1) and Table 2) and the measured saturated hydraulic conductivities. Therefore, Eqs. (2) and (3) were simply reported for the sake of completeness and they were not directly defined but were automatically generated on the basis of water retention models obtained from Eq. (1).

The predicted unsaturated hydraulic conductivity functions of all four materials are depicted in Fig. 6. According to this figure, the hydraulic conductivity of the naturally compacted soils is higher than the standard compacted ones at the low range of suction generally below the air entry value due to the difference in the initial void ratio and hence the saturated hydraulic conductivity at these two distinct compaction states. However, a sharp decrease in conductivity functions can be observed as suction increases. The important point is that conductivity functions of saline soils generally tend to decline at further suctions compared with their corresponding desalinated functions. Indeed, the higher water retention characteristics of saline soils play a significant role in delivering corresponding higher hydraulic conductivity functions. Therefore, it can be expected that flow under both steady-state and transient conditions is influenced by pore water salinity. Similar to the observations on water retention curves, results of Fig. 6 also suggest that the influence of salinity is much more pronounced on soils compacted with higher effort. Therefore, the stability of well-compacted soil embankment should be more affected by the existence of dissolved salts compared with that of natural loose soil stratum.

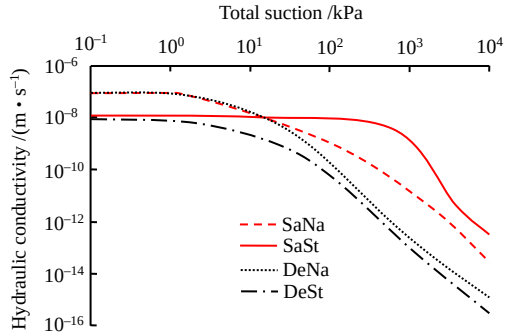

Fig. 6 Unsaturated hydraulic conductivity functions (HCF) of the four materials

3 Numerical study

3.1 Numerical model

In order to investigate the effect of dissolved salts on the stability of an unsaturated railway embankment under rainfall infiltration, series of numerical analyses are carried out based on the result of the experimental program presented in the previous section. These analyses comprise of two series of steady-state and transient seepage analyses using SEEP/W, and slope stability analyses using SLOPE/W software [31]. The finite element model used in this study is illustrated in Fig 7. According to this figure, the domain is divided into two sub-domains including the stratum with a height of 20 m, and a total width of 56 m, and the railway embankment with a standard slope of 1 to 2 (1 vertical, 2 horizontal) with a height of 5 m, and a width of 6 m for a single way railway line. It is noted that the geometry of the embankment is decided in accordance with the *National earthworks code for railway lines* [18]. Moreover, the element size of 0.5 m is selected according to a preliminary sensitivity analysis.

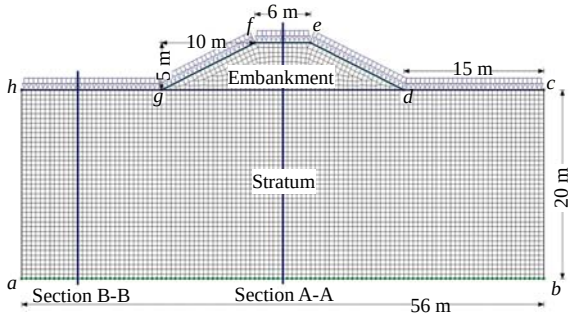

Fig. 7 Mesh, geometry, and the initial boundary conditions of the numerical model

3.2 Materials

Following the experimental study, four materials, including two types of saline and desalinated loess with two different states of compaction, are applied to the model in the numerical study. In order to examine the role of pore water salinity on flow characteristics and slope stability, two types of numerical modelling are simulated. The first type of numerical models comprises the saline loess with natural and standard compaction conditions for the stratum and the embankment, respectively. On the other hand, desalinated loess is considered as the studied material for the second type of analysis with the same regional compaction distribution as in the first numerical model. The soil strength properties of the saline loess, including its friction angle and cohesion for all materials, are summarised in Table 1. Although some previous researches show a slight increase in the soil friction angle by an increament in the salt solution[8–9], there is other research revealing that salinity do not have a considerable effect on the mechanical properties of the soil [32]. Therefore, the effect of salinity on the mechanical properties of materials is ignored in this study, and similar soil friction angle and cohesion are adopted for the desalinated loess.

3.3 Seepage analyses

It is well recognized that rainfall infiltration is the most important triggering mechanism of slope failure[2]. The general governing differential equation for two-dimensional water seepage through unsaturated soils can be written as:

$$\frac{\partial}{\partial x}\left(k_x\frac{\partial H}{\partial x}\right)+\frac{\partial}{\partial y}\left(k_y\frac{\partial H}{\partial y}\right)+Q=\frac{\partial \theta}{\partial t} \tag{4}$$

where H is the total head, k_x is the hydraulic conductivity in the x-direction, k_y is the hydraulic conductivity in the y-direction, Q is the applied boundary flux, θ is the volumetric water content, and t is time. According to Eq. (4), both hydraulic conductivity and water retention properties have a direct impact on the seepage through an unsaturated medium under transient flow. Under the steady-state conditions, on the other hand, the right-hand side term related to water retention characteristics vanishes and hydraulic conductivity becomes the key factor governing the water flow. In this study, rainfall infiltration is simulated by carrying out a two-step seepage simulation; at first, a steady-state analysis is carried out and afterwards, transient analyses are conducted to investigate the changes of pore water pressure in saline and desalinated medium.

The steady-state analysis was carried out to mimic the in-situ hydraulic conditions during field sampling as the initial conditions for numerical analyses. According to the subsurface exploration, the groundwater table was located 18 meters below the ground level. Such a deep groundwater table having a relatively high suction profile at surface layers was also reported for some natural loess stratum in semi-arid regions[33–34].

The *ab* boundry is a specified head boundary simulating the initial location of groundwater. The *cdefgh* is a specified flux boundary according to the simulated rainfal conditions. In addition, the derivative of hydraulic head with respect to the horizontal axis is considered zero along the both *bc* and *ha* boundaries. Details of boundary conditions representing the filed conditions are as follows. Regarding the steady-state analysis, a pressure head of 2 meters is applied to the

bottom of the model (line *ab* in Fig. 7), representing the depth of groundwater table, and a very low-intensity rainfall (0.01 mm/d) is applied to the whole surface of the model (line *cdefgh* in Fig. 7). Following the steady-state analysis, the transient analysis is carried out with a medium-intensity rainfall. According to the meteorological data of the region, the total amount of rainfall at the study area in the winter (wet season) is 87.2 mm. Therefore, a medium-intensity rainfall with a duration of 5 days and the intensity of 17.4 mm/d is applied to the model after the steady-state analysis.

3.4 Slope stability analysis

Slope stability analyses are carried out after the seepage analyses to calculate the factor of safety against slope failure. The limit equilibrium method proposed by Spencer [35] for solving the equilibrium equations is used for calculating the factor of safety. In addition, the impact of measured SWRCs is highlighted by incorporating the relevant water retention properties in the estimation of the soil shear strength[36]. The widely used modified Mohr-Coulomb equation proposed by Vanapalli et al. [37] is used accordingly:

$$\tau_{\mathrm{ff}} = c' + (\sigma_{\mathrm{f}} - u_{\mathrm{a}})_{\mathrm{f}} \tan\varphi' + (u_{\mathrm{a}} - u_{\mathrm{w}})_{\mathrm{f}} \left(\frac{\theta - \theta_{\mathrm{r}}}{1 - \theta_{\mathrm{r}}} \right) \tan\varphi' \tag{5}$$

where τ_{ff} is the shear strength at the failure, σ_{f} is the normal stress at the failure, u_{a} is air pressure, and u_{w} is water pressure. When dissolved salts in pore fluid diffuse to the clay surface, the effective stress formulation of Terzaghi should be extended to consider both the electrostatic repulsive pressure, and the van der Waals force. This is due to the fact that previous studies revealed the significant role of osmotic suction on mechanical properties of clayey soils[8–9]. On the other hand, some other studies indicated that shear strength is almost independent of osmotic suction[32]. In order to clarify this issue, six direct shear tests were conducted on both saline and desalinated soil specimens consolidated to three different normal stresses. The results of Fig. 8 confirm that both shear failure envelopes are in a good agreement. In other words, the influence of osmotic suction on saturated shear strength is almost negligible for the low plastic clay used in this study. As a result, the only variable governing the unsaturated shear strength of tested soil is soil–water retention curve not osmotic suction. Therefore, the saturated soil strength parameters corresponding to different compaction states are selected from Table 1. Furthermore, the initial density of the materials is calculated based on the initial water content at the beginning of the analysis. As rainfall proceeds, the value of soil density is updated based on the spatial changes in the degree of saturation over the studied domain. In addition, the total track and train loads are assumed to be 170 kPa, based on the allowable subgrade bearing capacity of the embankment[38].

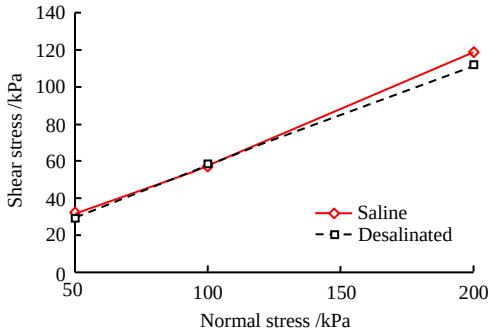

Fig. 8 Shear stress vs. normal stress of both saline and desalinated materials

3.5 Interpretation of the results

3.5.1 Volumetric water content distribution

The variations in volumetric water content of saline and desalinated models at different time intervals from the rainfall initiation are illustrated in both embankment and the stratum in Fig. 9. Figs 9(a) and 9(b) show the results of the embankment along section A-A (Fig. 7) for saline and desalinated models, respectively. According to Fig. 9(a), the volumetric water content of the saline embankment increases from the initial condition during the five days of rainfall, and after that, it gradually decreases. In addition, it is evident that water gradually infiltrates the embankment and reaches its bottom after three days. This type of water flow regime arises from the highest water retention properties, and unsaturated conductivity function of the standard compacted saline loess measured previously. On the contrary, the results of Fig. 9(b) confirm that water cannot readily infiltrate into the desalinated embankment due to the very low rate of the hydraulic conductivity coupled with relatively lower water retention compared with saline soil. As a result, water cannot reach the bottom of the embankment as most of the input rainfall runs off through the surface of the embankment. Variations in the volumetric water content of the stratum along section B-B up to 5 m down the ground surface are depicted in Figs 9(c) and 9(d) for saline and desalinated models, respectively. According to the results, an almost similar pattern in flow characteristics can be interpreted for the stratum with a relatively lower dry density as compared with the embankment. Although the stratum has a higher hydraulic conductivity in comparison with the embankment, salinity plays a major role in facilitating water infiltration into the naturally compacted soil. In other words, water hardly can infiltrate into the desalinated stratum due to the lower retention ability.

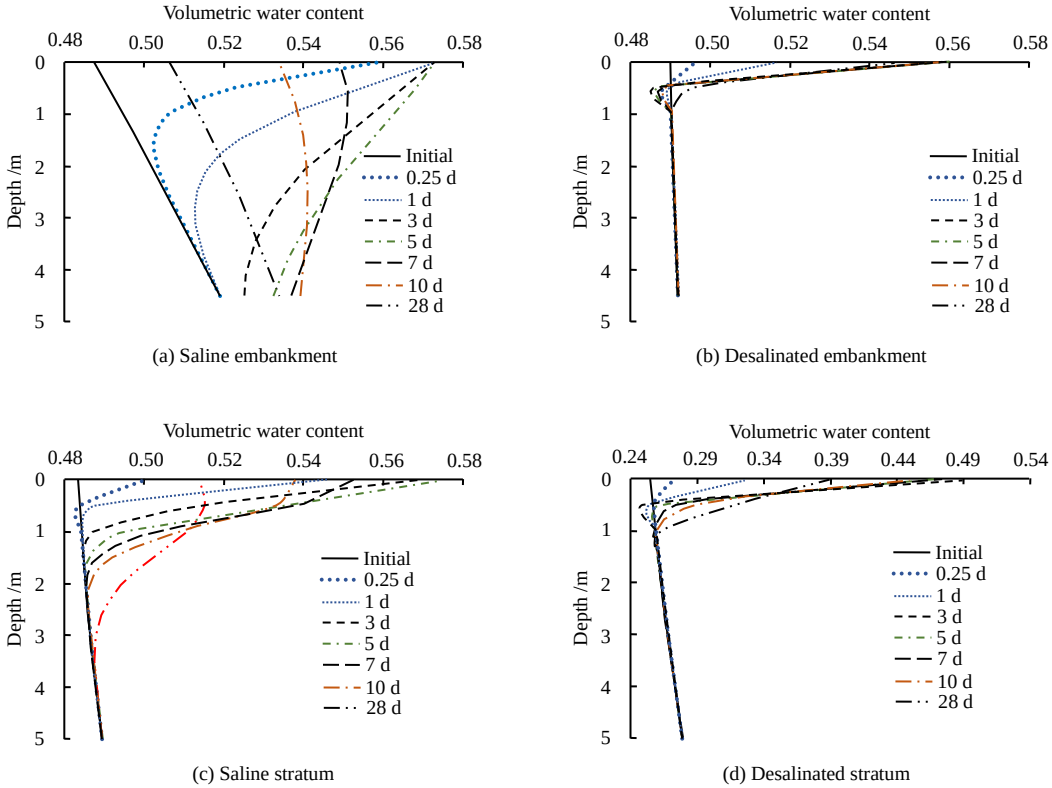

Fig. 9 Distribution of volumetric water content

3.5.2 Factor of safety

Figure 10 indicates the variations in the factor of safety during and after the rainfall incident for both saline and desalinated models. It should be mentioned that light blue shadow in the figure represent the period of applied rainfall. According to the results, the factor of safety of saline model significantly decreases during the rainfall and gradually increases after that. During the rainfall, soil suction and therefore, soil strength decreases due to the increment of the degree of saturation, and it leads to a sharp drop in the factor of safety against stability. Meanwhile, the rise in the degree of saturation also contributes to the enhancement of driving potential, which in turn results in an accelerated rate of reduction in the factor of safety. As rainfall stops, however, the pore water pressure starts to dissipate, and the magnitude of soil suction increases. Consequently, a mild recovery of the factor of safety with time can be observed.

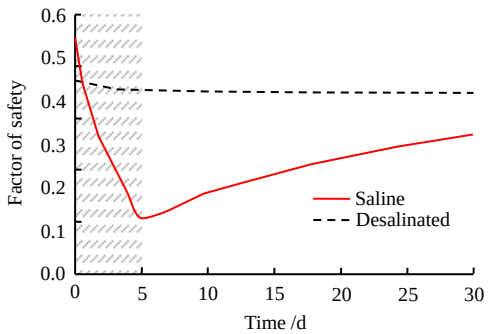

Fig. 10 Variation of factor of safety with time in saline and desalinated models during and after the rainfall

On the other hand, the factor of safety of the desalinated model hardly changes during and after the rainfall infiltration, due to the relatively lower hydraulic conductivity compared with saline loess (Fig. 10). As shown in Figs. 8(b) and 8(d), the desalinated model behaves as it is more impervious to rainfall infiltration compared with the saline model. Therefore, water can hardly infiltrate into the desalinated model, and the factor of safety against stability is marginally influenced by rainfall precipitation for the modelling conditions considered in this study. Based on comparisons made in Fig. 10, it can be concluded that the factor of safety of the saline soil is much more influenced by rainfall, and hence is considered more critical than the corresponding values of the desalinated soil. From the suction perspective, one may conclude that the osmotic suction induced by dissolved ions and salts in natural soils can cause a significant drop in the factor of safety against the stability of the railway embankment. In other words, the osmotic potential is responsible for severe failure captured in Fig. 2 although the embankment was heavily compacted to the experimentally determined maximum dry density but with natural salinity.

4 Parametric study

A parametric study was carried out to investigate the role of crucial factors on the stability of the embankment. In this regard, the effect of rainfall intensity and duration was explored through conducting a series of analyses with three different rainfall patterns. Afterwards, the influence of construction pattern with

emphasis on nil and raised salinity of embankment and stratum for all possible combinations were investigated. Eventually, the impact of anisotropy in hydraulic conductivity on the factor of safety was examined.

4.1 Effect of rainfall pattern

Rainfall patterns are one of the controversial factors that are widely investigated through slope stability analysis [39]. In previous research, the main factors considered in exploring the rainfall influence on the slope stability included total rainfall amount (mm), rainfall intensity (mm/d), and the rainfall duration (d). As the total amount of the rainfall in this study, i.e. 87.2 mm, was extracted from the real national meteorological database [40], rainfall intensity and duration were simply considered for the parametric study. Three different rainfall patterns with the same total rainfall amount of 87.2 mm were applied to both saline and desalinated models; details of which are summarized in Table 3. It is worth mentioning that these patterns were decided based on possible meteorological events.

Table 3 Details of the three rainfall patterns

Index	Intensity /(mm • d^{-1})	Duration /d	Total amount of rainfall /mm
LI	8.7	10	
MI	17.4	5	87.2
HI	43.6	2	

Note: LI is low-intensity, MI is medium-intensity, and HI is high-intensity.

Results of the spatial distribution of volumetric water content along section A-A of the saline embankment are illustrated in Fig. 11 at the end of each rainfall scenario. The initial distribution is also depicted as a benchmark for comparison. According to the results, the wet front advances remarkably under the low-intensity rainfall while the application of the high-intensity pattern results in the slowest advancement of the wet front. Accordingly, the duration of the rainfall plays a significant role in the relative proportioning of run-off and permeated water. For the material properties considered in this study, rainwater can more effectively infiltrate into the embankment under the lowest intensity. The implication is hence that a greater portion of the embankment suffers from suction loss.

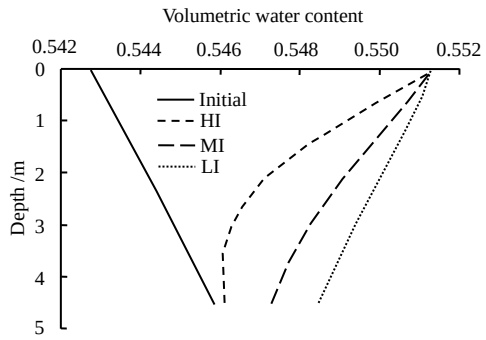

Fig. 11 Volumetric water content distribution of saline embankment at the end of HI, MI, and LI rainfall patterns

Figure 12 demonstrates the variations in the factor of safety with time during and after the rainfall for various rainfall patterns. According to Fig. 12(a), the factor of safety of saline model is considerably influenced by the rainfall intensity. The low-intensity rainfall resulted in the most significant drop in the factor of safety compared with the other cases. The fact that the application of low-intensity rainfall is the most crucial scenario amongst others was also expected from the spatial distribution of water content discussed in Fig. 11. On the other hand, rainfall pattern has similar effects on the stability of the desalinated model, although the influence is much more insignificant compared with the case of the saline model (Fig. 12(b)). Moreover, another distinction between the trends of variations in the factor of safety for two models considered is that the factor of safety corresponding to desalinated model continuously decreases even after the rainfall at a reduced rate and there is no sign of recovery, similar to the case of the saline model. This observation suggests that low dissipation rate of desalinated model arises from water retention properties does not allow the factor of safety to recover promptly after the termination of the rainfall incident.

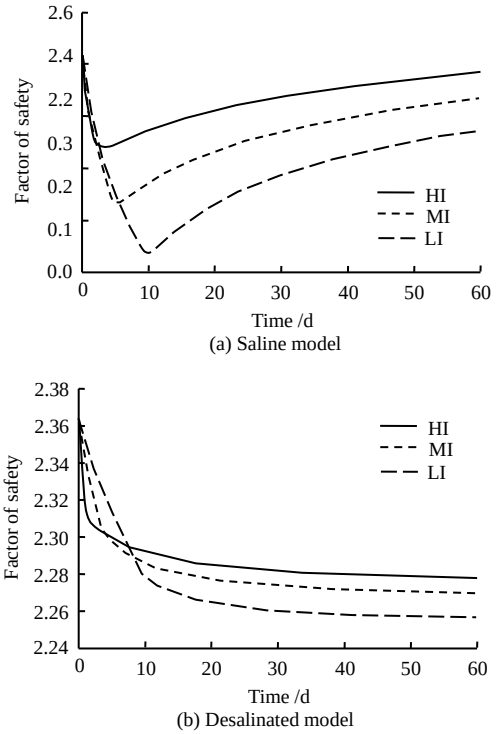

Fig. 12 Effect of rainfall pattern on the factor of safety

4.2 Effect of construction patterns in terms of natural salinity

In order to explore how the pattern of constructing embankment and stratum from saline or desalinated soils might affect the stability, the second series of the parametric study was carried out considering all four possible combinations. The studied models included two completely saline and desalinated models and another two with alternate salinity conditions for the embankment and the stratum. The main purpose of

these series of analysis was to provide a practical guideline and the best solution for constructing embankment on the natural saline environment in case of the budget constraint. The construction details and simulation identity of the four analyses carried out are summarized in Table 4. It is noted that according to the observations made on the influence of rainfall pattern, the low-intensity rainfall infiltration was considered as the most crucial scenario in the analyses.

Table 4 Details of four salinity models

ID	Embankment salinity	Stratum salinity
SS	Saline	Saline
DD	Desalinated	Desalinated
SD	Saline	Desalinated
DS	Desalinated	Saline

The factor of safety of all DS, DD, SS, and SD numerical models under the low-intensity rainfall pattern is depicted and compared in Fig. 13. According to this figure, the factor of safety of SS and SD models reduced more significantly than the other two models during the rainfall and increased afterwards in spite of the other two cases where the reduction was continuous and less pronounced. Of particular interest is the case of DS numerical model where the embankment is constructed with desalinated soil and founded on the natural saline stratum. Comparisons of results reveal that following this specific construction pattern, the highest factor of safety could be obtained. Therefore, this case might be considered as the most conservative yet economical practical solution where osmotic suction exists in the natural stratum.

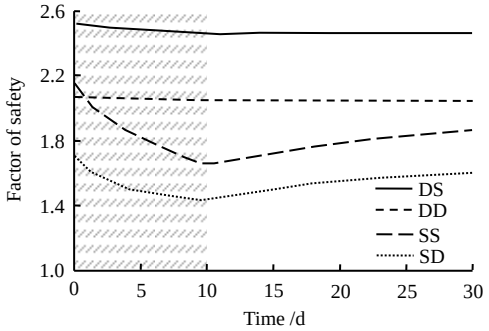

Fig. 13 Variations of factor of safety for DS, DD, SS, SD models during and after the LI rainfall

Comparisons between the results of two saline embankment cases (SS and SD) with the other two desalinated ones (DS and DD) in Fig. 13 also indicate that in spite of the former, the factor of safety corresponding to the latter cases hardly diminishes during and even after the rainfall. The implication is that the material type used for the embankment should play a more prominent role in the stability compared with the type of material used in the stratum. In other words, the saline embankment is much more critical than the saline stratum, and the osmotic potential of the embankment has a greater influence on the overall stability of the model.

4.3 Effect of anisotropy

Anisotropy of hydraulic conductivity is one of the most imperative factors, which can adversely affect the stability of slopes[39]. However, in order to simplify the modelling procedure, it is usually ignored in flow models and slope stability analysis[41–42]. In the current study, the last series of the parametric study was conducted to examine the effect of anisotropy on the stability of the embankment. Therefore, three different cases were assumed for both saline, and desalinated models, including the ratios of horizontal to vertical hydraulic conductivities (k_x/k_y), of 1, 2 and 4.

Figure 14 indicates the initial pore water pressure distribution in the saline model along the symmetry axis (A-A) for the three different anisotropic hydraulic conductivities at the steady-state condition. According to this figure, as the anisotropy increases, the pore water pressure also increases, and it brings about lower suction ranges in the soil profile. This might be explained by the low rate of hydraulic conductivity in the *y*-direction at higher anisotropy ratios, which in turn results in a higher ratio of Q/k_y in Eq. (4). Therefore, the initial very low-intensity rainfall better infiltrates into the soil at a higher anisotropy ratio and induces the suction of the soil to decline [39]. Fig. 15 indicates the variations in the factor of safety with time for different anisotropic saline and desalinated models. According to this figure, the factor of safety of the models with the anisotropy ratio of 4 is the worst-case scenario for both saline and desalinated models. As suction loss accelerated by enhancement of the anisotropy ratio, it can be expected that the soil strength diminishes and brings about a lower factor of safety. Additionally, it can be inferred from the results that by increasing the anisotropy, the rate of recovery in the factor of safety with time also declines. Fig. 16 compares the factor of safety corresponding to the saline models constructed with different anisotropy ratios and subjected to three different rainfall patterns.

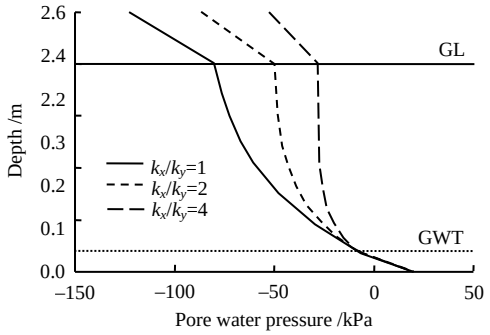

Fig. 14 Anisotropy effect on the pore water pressure distribution of saline model at the initial condition (GL: ground level, GWT: groundwater table)

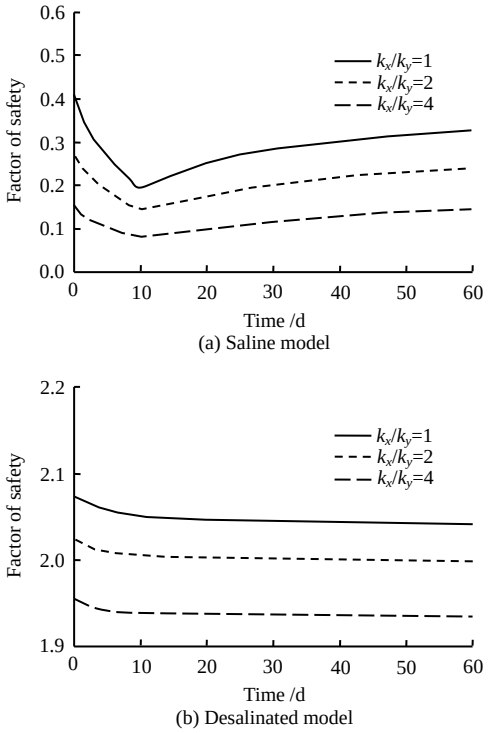

Fig. 15 Anisotropy effect on the factor of safety

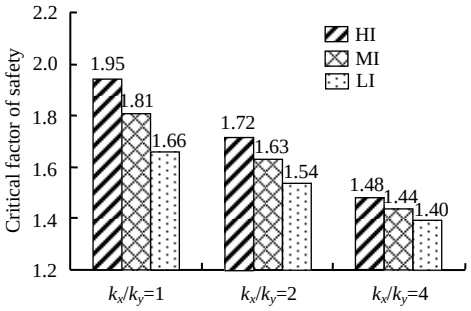

Fig. 16 Anisotropy effect on the critical factor of safety of the saline model under different rainfall patterns

According to the results, by increasing the anisotropy ratio, the influence of the rainfall infiltration decreases. In other words, at the isotropic state, the difference between the factor of safety under HI and LI rainfalls is 0.29, while this difference for the anisotropy ratio of 4 reduces to 0.08. Similarly, the observed discrepancy can also be explained by the rationale used for explaining the variations in pore water pressure with the anisotropy ratio.

5 Summary and conclusions

A combined methodology of laboratory experiments and numerical simulations was adopted to provide insight into the stability of a railway embankment crossing natural loess strata with distinct pore water salinity. The contact and non-contact types of filter paper tests were carried out on natural saline and artificially desalinated in-situ soils to infer all suction components, including the osmotic potential. In addition, the saturated hydraulic conductivity of both materials was measured and used in conjunction with water retention data to derive unsaturated hydraulic conductivity functions for flow analyses. The experimental results revealed that the water retention ability of the saline loess is much more than the desalinated one, leading to a generally higher conductivity function for the saline soil. Regarding the numerical study, results indicated that the factor of safety of the saline model dramatically dropped during the rainfall and started to recover at the end of the rainfall; however, the factor of safety of the desalinated model was almost insensitive to rainfall incident for the examined slope conditions. Looking into the transient changes in the volumetric water content, it was confirmed that lower water retention and conductivity of desalinated soils prevented the rainwater from infiltrating into the embankment readily, so surface run-off was dominant in this case. On the other hand, a higher amount of precipitation was absorbed by saline embankment due to its relatively higher water retention and conductivity properties. This, in turn, resulted in the generation of pore water pressure, and hence a much lower factor of safety was obtained. Pore water salinity, indeed, was shown to endanger the stability of a slope being designed conservatively neglecting the role of osmotic potential. Of particular interest is the results of the parametric study on the influence of construction pattern on stability state. According to the results, the highest factor of safety can be obtained for the desalinated embankment constructed on the natural saline stratum, while the mutual exchange of material types resulted in the worst-case scenario. In addition, the rainfall intensity had an adverse impact on the stability of both types of embankment. In other words, the factor of safety diminished more as the intensity of the rainfall reduced. On the other hand, a lower factor of safety was calculated as a higher anisotropic ratio of hydraulic conductivity was assigned to the models.

The increased rate of pollution released to the environment as a consequence of industrialization results in limited access to fresh water or counter-measure against pollution transport [43–44]. It seems therefore necessary to revisit the classic measurements and simulation based on pure water permeation through soil media. Although some simplified aspects of such geoenvironmental problems were explored in this study, some other physio- chemical aspects such as the transport of salt species were ignored [45]. In other words, only Darcian flow type was considered in this study while chemico- osmosis type of flow arise from concentration gradient was ignored. Therefore, further studies are required to provide insight into the

coupled multiphase flow phenomena through soil.

Declaration of competing interest

The authors declare that they have no known competing financial interests or personal relationships that could have appeared to influence the work reported in this paper.

Acknowledgment

Aurhors would like to thank Mr. Pouya AliPanahi for conducting some complementary shear test experiments. The first author is also greatful to the Iran's National Elites Foundation and the Research Grant Office at Sharif University Technology for supporting this research by way of "*Dr Kazemi-Ashtiani Award*" and grant "*G970902*", respectively.

References

[1] HOU X, VANAPALLI S K, LI T. Water infiltration characteristics in loess associated with irrigation activities and its influence on the slope stability in Heifangtai loess highland, China[J]. Engineering Geology, 2018, 234: 27–37.

[2] ZHANG L L, ZHANG J, ZHANG L M, et al. Stability analysis of rainfall-induced slope failure: a review[J]. Geotechnical Engineering, 2011, 164(5): 299–316.

[3] WEN B P, YAN Y J. Influence of structure on shear characteristics of the unsaturated loess in Lanzhou, China[J]. Engineering Geology, 2014, 168: 46–58.

[4] SADEGHI H, KIANI M, SADEGHI M, et al. Geotechnical characterization and collapsibility of a natural dispersive loess[J]. Engineering Geology, 2019, 250: 89–100.

[5] SADEGHI H, DARZI A G. Modelling of soil-water retention curve considering the effects of existing salt solution in the pore fluid[C]//MATEC Web of Conferences. [S. l.]: EDP Sciences, 2021.

[6] THYAGARAJ T, SALINI U. Effect of pore fluid osmotic suction on matric and total suctions of compacted clay[J]. Géotechnique, 2015, 65(11): 952–960.

[7] HE Y, YE W M, CHEN Y G, et al. Influence of pore fluid concentration on water retention properties of compacted GMZ01 bentonite[J]. Applied Clay Science, 2016, 129: 131–141.

[8] DI MAIO C. Exposure of bentonite to salt solution: osmotic and mechanical effects[J]. Géotechnique, 1996, 46(4): 695–707.

[9] DI MAIO C, SCARINGI G. Shear displacements induced by decrease in pore solution concentration on a pre-existing slip surface[J]. Engineering Geology, 2016, 200: 1–9.

[10] SREEDEEP S, SINGH D N. Critical review of the methodologies employed for soil suction measurement[J]. International Journal of Geomechanics, 2011, 11(2): 99–104.

[11] MA T, WEI C, XIA X, et al. Soil freezing and soil water retention characteristics: connection and solute effects[J]. Journal of Performance of Constructed Facilities, 2017, 31(1): D4015001.

[12] ZHANG Y, YE W, CHEN Y, et al. Impact of NaCl on drying shrinkage behavior of low-plasticity soil in earthen heritages[J]. Canadian Geotechnical Journal, 2017, 54(12): 1762–1774.

[13] GARAKANI A A, HAERI S M, CHERATI D Y, et al. Effect of road salts on the hydro-mechanical behavior of unsaturated collapsible soils[J]. Transportation Geotechnics, 2018, 17: 77–90.

[14] FREDLUND D G, RAHARDJO & H, FREDLUND M D. Unsaturated soil mechanics in engineering practice[M]. New York: Wiley, 2012.

[15] BAZARGAN A, SADEGHI H, GARCIA-MAYORAL R, et al. An unsteady state retention model for fluid desorption from sorbents[J]. Journal of Colloid and Interface Science, 2015, 450: 127–34.

[16] HOSSEINI S A, MOJTAHEDI S F, SADEGHI H. Optimisation of deep mixing technique by artificial neural network based on laboratory and field experiments[J]. Georisk: Assessment and Management of Risk for Engineered Systems and Geohazards, 2020, 14(2): 142–57.

[17] SADEGHI H, NASIRI H, ALIPANAHI P, et al. Dispersivity, collapsibility, and microstructure of a natural dispersive loess from Iran[C]//Proceedings of the 16th Asian Regional Conference on Soil Mechanics and Geotechnical Engineering. Taibei(Taipei): [s. n.], 2019.

[18] Management and Planning Organization Office of Deputy for Technical Affairs, Technical Criteria and Specification Bureau, National earthworks code for railway lines[S]. [S. l.]: [s. n.], 2004.

[19] ZHANG Y, YE W M, CHEN B, et al. Desiccation of NaCl contaminated soil of earthen heritages in the Site of Yar City, northwest China[J]. Applied Clay Science, 2016, 124: 1–10.

[20] SADEGHI H. A micro-structural study on hydro-mechanical behavior of loess[D]. Hong Kong & Tehran: The Hong Kong University of Science and Technology & Sharif University of Technology, 2016.

[21] ASTM. Annual book of ASTM standards[M]. West Conshohocken, Pa: ASTM International, 2009.

[22] SADEGHI H, HOSSEN S B, CHIU A C, et al. Water retention curves of intact and re-compacted loess at different net stresses[J]. Japanese Geotechnical Society Special Publication, 2016, 2(4): 221–5.

[23] PHAM H Q, FREDLUND D G. Equations for the entire

soil-water characteristic curve of a volume change soil[J]. Canadian Geotechnical Journal, 2008, 45(4): 443–453.

[24] GOLAGHAEI DARZI A A, SADEGHI H. Review of different approaches to analytical modeling of soil-water retention curves[J]. Sharif Journal of Civil Engineering, 2021. DOI: 10.24200/j30.2021.56932.2870.

[25] SADEGHI H, NASIRI H. Hysteresis of soil water retention and shrinkage behaviour for various salt concentrations[J]. Géotechnique Letters, 2021, 11(1): 21–29.

[26] NG C W W, SADEGHI H, HOSSEN S K B, et al. Water retention and volumetric characteristics of intact and re-compacted loess[J]. Canadian Geotechnical Journal, 2016, 53(8): 1258–1269.

[27] SADEGHI H, CHIU A C, NG C W, et al. A vacuum-refilled tensiometer for deep monitoring of in-situ pore water pressure[J]. Scientia Iranica, 2020, 27(2): 596–606.

[28] SADEGHI M, SADEGHI H, CHOI CE. A lattice Boltzmann study of dynamic immiscible displacement mechanisms in pore doublets[C]//MATEC Web of Conferences. [S. l.]: [s. n.], EDP Sciences, 2021.

[29] FREDLUND M D, WILSON G W, FREDLUND D G. Use of the grain-size distribution for estimation of the soil-water characteristic curve[J]. Canadian Geotechnical Journal, 2002, 39(5): 1103–1117.

[30] SADEGHI H, ALIPANAHI P. Saturated hydraulic conductivity of problematic soils measured by a newly developed low-compliance triaxial permeameter[J]. Engineering Geology, 2020, 278, 105827.

[31] GARAKANI A A, BIRGANI M M, SADEGHI H. An effective stress-based parametric study on the seismic stability of unsaturated slopes with implications for preliminary microzonation[J]. Bulletin of Engineering Geology and the Environment, 2021, 80(10): 7525–49.

[32] LEONG E C, ABUEL-NAGA H. Contribution of osmotic suction to shear strength of unsaturated high plasticity silty soil[J]. Geomechanics for Energy and the Environment, 2018, 15: 65–73.

[33] NG C W W, SADEGHI H, JAFARZADEH F, et al. Effect of microstructure on shear strength and dilatancy of unsaturated loess at high suctions[J]. Canadian Geotechnical Journal, 2020, 57(2): 221–235.

[34] SADEGHI H, NG CW. Shear behaviour of a desiccated loess with three different microstructures[C]//7th International Conference on Unsaturated Soils. Hong Kong: [s. n.], 2018, 1(401): 1–6.

[35] SPENCER E. A method of analysis of embankments assuming parallel inter-slice forces[J]. Géotechnique, 1967, 17(1): 11–26.

[36] AKBARI GARAKANI A, SADEGHI H, SAHEB S, et al. Bearing capacity of shallow foundations on unsaturated soils: analytical approach with 3D numerical simulations and experimental validations[J]. International Journal of Geomechanics, 2020, 20(3): 04019181.

[37] VANAPALLI S K, FREDLUND D G, PUFAHL D E, et al. Model for the prediction of shear strength with respect to soil suction[J]. Canadian Geotechnical Journal, 1996, 33(3): 379–392.

[38] SELIG E T, WATERS J M, AYERS M E, et al. Track geotechnology and substructure management[J]. 1978, 8: 16-26.

[39] NG C W W, SHI Q. A numerical investigation of the stability of unsaturated soil slopes subjected to transient seepage[J]. Computers and Geotechnics, 1997, 22(1): 1–28.

[40] DEPATMENT M. Iran Meteorological Organization[EB/OL]. (2019-07-31)[2022-01-25]. http://www.irimo.ir/ eng/index.php.

[41] GARAKANI A A, BIRGANI M M, SADEGHI H. Semi-empirical modelling of hydraulic conductivity of clayey soils exposed to deionized and saline environments[J]. Journal of Contaminant Hydrology, 2022, 249: 104042.

[42] LE T M H, GALLIPOLI D, SÁNCHEZ M, et al. Stability and failure mass of unsaturated heterogeneous slopes[J]. Canadian Geotechnical Journal, 2015, 52(11): 1747–1761.

[43] KHADIR A, RAMEZANALI A M, TAGHIPOUR S, et al. Insights of the removal of antibiotics from water and wastewater: a review on physical, chemical, and biological techniques[M]//Applied Water Science. [S. l.]: [s. n.], Technologies, 2021.

[44] TAGHIPOUR S, KHADIR A, TAGHIPOUR M. Carbon nanotubes composite membrane for water desalination[C]// Sustainable Materials and Systems for Water Desalination. Cham: Springer, 2021.

[45] HEDAYATI-AZAR A, SADEGHI H. A review of research approaches to contaminant transport in saturated deformable clay under coupled hydro-chemico-mechanical processes[J]. Sharif Journal of Mechanical Engineering, 2021. DOI: 10.24200/J40.2021.56928.1565.